THE JOURNAL OF PHYSICAL CHEMISTRY C

ARTICLE

pubs.acs.org/JPCC

Defect-Mediated Energy Transfer between ZnO Nanocrystals and a Conjugated Dye

Gary A. Beane,[†] Anthony J. Morfa,[†] Alison M. Funston,[‡] and Paul Mulvaney*[,†]

[†]School of Chemistry & Bio21 Institute, University of Melbourne, Parkville, Victoria 3010, Australia

[‡]School of Chemistry, Monash University, Clayton, Victoria 3800, Australia

Supporting Information

ABSTRACT: Energy transfer from the defect state of zinc oxide nanoparticles to the fluorescent dye AlexaFluor 594 (A594) cadaverine has been studied using both steady-state and time-resolved photoluminescence (PL) measurements. The addition of five stoichiometric equivalents of A594 cadaverine completely quenches the visible defect emission from zinc oxide nano crystals. We also find that the entire defect emission of ZnO is reduced without any change in the overall line shape of the emission, demonstrating that the defect emission is from a single electronic state coupled to the phonon modes of the crystal lattice. The energy transfer is modeled using the dynamic quenching model developed by Tachiya (Sadhu, S.; Tachiya, M. *J. Phys. Chem.* **2009**, *113*, 19488−19492). Remarkably, there is very efficient energy transfer when there is just one adsorbed dye molecule per nanocrystal, regardless of the orientation of the dipole moment of the cadaverine molecule and the distance to the defect state.

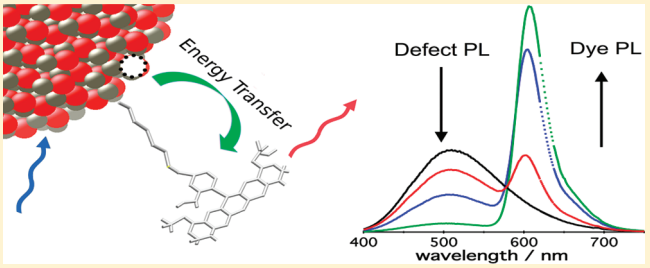

INTRODUCTION

The quenching of exciton emission in semiconducting nanocrystals by fluorophores has been studied extensively over the past decade.[1−7] These reports have focused overwhelmingly on energy transfer from the exciton state of the nanocrystals. To date, there have been no systematic studies of energy transfer from charge carriers in defect or trap states of nanocrystals to acceptors. Such studies are important because surface and defect recombination limits the overall radiative quantum yield of a semiconductor nanocrystal. In some cases, the defect emission may even dominate over exciton emission. For example, under UV irradiation, the semiconductor ZnO displays an intense green emission that overwhelms the UV exciton emission of the nanocrystal.[8] The decrease in intensity of the defect emission upon annealing of ZnO films suggests that vacancies within the crystals play a role in the emission,[9] whereas the dependence of the visible emission band energy on the particle size[10−12] implies that a delocalized charge carrier is involved in the emission process. That, in turn, suggests that there will be a large dipole moment change associated with trap emission and that energy transfer to fluorophores should be possible.

The broad visible emission observed in ZnO has been attributed variously to interstitial zinc ions,[13] oxygen vancancies,[14] chemisorbed oxygen,[15] divalent copper impurities,[16] and zinc vacancies.[17] Presently, oxygen vacancies are thought to be the likely cause of the visible emission.[18−21] The review paper by Ozgür et.al. provides an excellent overview of the main models.[22]

Whereas the nature of the defect emission continues to be debated, there have been recent reports that have implicated the defect state as an energy-transfer donor species with organic fluorophores.[23−27] However, calculations of the donor−acceptor dipole moments (using the Forster resonance energy transfer formalism) have yielded contradictory results. For example, energy transfer from defect states located close to the nanocrystal surface were proposed to explain the unexpectedly small donor−acceptor distance when the dye was covalently linked.[26,27] In contrast, when the dye was not covalently linked, surface states were not explicitly required to explain the measured donor−acceptor distance, although defect states were proposed as the energy donor.[24] Hence, the general applicability of the Forster mechanism to energy transfer involving surface states must be in doubt. Another important issue is that nanocrystal defect emission is known to be sensitive to surface chemistry.[28−32] For example, carboxyl-containing molecules can be photocatalytically decomposed by ZnO.[33,34] Hence it is important to separate quenching due to energy transfer from quenching due to photochemical processes of the adsorbates.

In this Article, we present evidence of very efficient energy transfer between ZnO and Alexa594 cadaverine (A594 cadaverine) using steady-state and time-resolved photoluminescence (PL) measurements. We find that the observed quenching is caused by adsorbed dye molecules and that this quenching is due to energy transfer from ZnO defect states rather than the ZnO exciton state. Using the Tachiya model, we calculate that even a single dye molecule can effectively quench the emission,

Received: October 6, 2011
Revised: December 16, 2011
Published: December 27, 2011

although a mole ratio of five dyes per nanocrystal is needed to quench >95% of the ensemble PL due to the Poisson distribution of dye molecules among the ZnO nanocrystals. This is remarkable because the dipole moment of the adsorbed dye will not always be favorable for transfer.

EXPERIMENTAL SECTION

Synthesis of ZnO Nanocrystals. ZnO nanoparticles were prepared via the method of Wood et al.[12] In brief, zinc acetate dihydrate (0.955 g) was dissolved in 100 mL of absolute ethanol to make a total solute concentration of 44 mM. Upon complete dissolution of zinc acetate, seven 400 μL aliquots (2.8 mL total) of 25% w/w tetramethyl ammonium hydroxide in methanol was added over ca. 120 s with vigorous stirring in a water bath at 25 °C. The ZnO nanoparticle solution was then placed in a freezer maintained at −4 °C and stored until use. Solvents were sourced from Sigma-Aldrich and were either HPLC or spectroscopic grade for the fluorescence measurements. Alexa 594 cadaverine and rhodamine 6G (Rh6G) were purchased from Invitrogen and Exciton, respectively, whereas aminopentanol (95%) was purchased from Aldrich; all chemicals were used as received.

Sample Preparation. The diameter of ZnO nanoparticles in the as-synthesized solution was determined to be 3.2 nm using the calibration curve of Wood et al.[12] Concentrations were calculated assuming the formation of particles of this size and assuming complete conversion of precursors into particles. Samples for fluorescence measurements were all prepared in ethanol (HPLC grade, Sigma-Aldrich). For steady-state emission experiments, the samples had a ZnO concentration of 212 nM and an A594 cadaverine concentration of 0−1060 nM; the absorbance of the sample at the excitation wavelength was <0.1. All samples were left to equilibrate following mixing of the ZnO and A594 cadaverine for 5 min prior to measurements and were not degassed. The quantum yield of ZnO was measured with respect to a Rh6G standard under a N_2 atmosphere. For PL measurements, the excitation wavelength was 314 nm, and the quantum yield of Rh6G at this wavelength was taken to be 0.95.[35]

Instrumentation. UV−visible absorbance spectra were collected using an Agilent 8453 UV−visible absorbance spectrophotometer system. PL spectra were obtained using a Horiba Jobin Yvon Fluorolog-3 with an excitation wavelength of 314 nm. Time-resolved emission measurements were carried out with excitation at 300 nm using a Picoquant NanoLED-300 pulsed diode laser with detection at a wavelength of 500 nm. The instrument response of the system was measured using a colloidal silica dispersion in water with an absorbance of 0.1 at 300 nm and had a full width half-maximum (fwhm) of 2.0 ns.

RESULTS

Optical Absorbance. The photophysical characteristics of the species used in this study are summarized in Table 1, whereas the optical absorbance and emission spectra of ZnO nanocrystals and A594 cadaverine are shown in Figure 1.

The sharp ZnO exciton absorbance at 314 nm (3.96 eV) is consistent with a narrow size distribution and a particle size

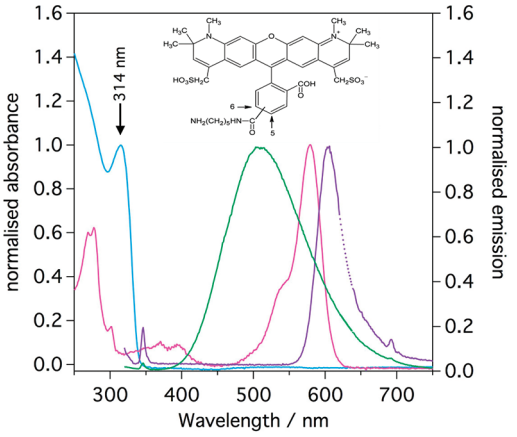

Figure 1. Normalized absorbance spectra of ZnO (light blue) and A594 cadaverine (light purple) along with the normalized emission of ZnO (green) and A594 cadaverine (dark purple) in ethanol. The optical absorption of the ZnO band-edge exciton is apparent at 314 nm (3.96 eV) while the emission of this state is not evident. The ZnO visible trap emission has a maximum at 510 nm (2.44 eV). Inset shows the structure of the dye A594 cadaverine. Rayleigh scattering and its second harmonic occur at 340 and 680 nm in the emission spectra. The second harmonic of the excitation wavelength (628 nm) has been removed for clarity, and the dotted lines in the emission spectra represent fits to the emission line shape. Excitation was at a wavelength of 314 nm.

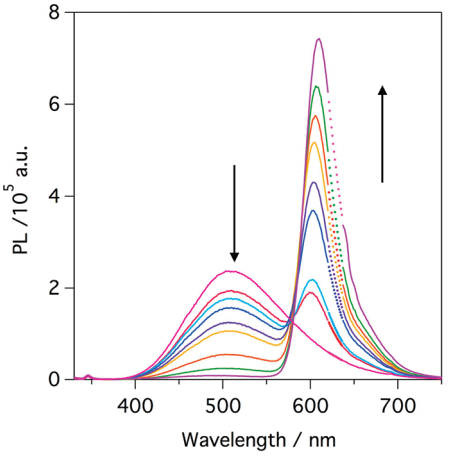

Figure 2. Emission spectra of ethanolic solutions containing 212 nM zinc oxide with increasing concentrations of A594 cadaverine, from top to bottom on the left of the Figure, 0−1060 nM. Excitation was at a wavelength of 314 nm.

Table 1. General Photophysical Properties of the Different Chemical Species Used[a]

	$\lambda_{abs,max}$ (nm)	$\lambda_{em,max}$ (nm)	ε (314 nm) ($M^{-1}cm^{-1}$)	τ (ns)	QY
ZnO (D = 3.2 nm)	314	510	5.56×10^5	588.1	0.12
A594	591	610	349	4.6	0.66[36]
Rh6G	529	553	27.0		0.95[35]

[a] All data are for species in ethanol.

dx.doi.org/10.1021/jp209638g |J. Phys. Chem. C 2012, 116, 3305–3310

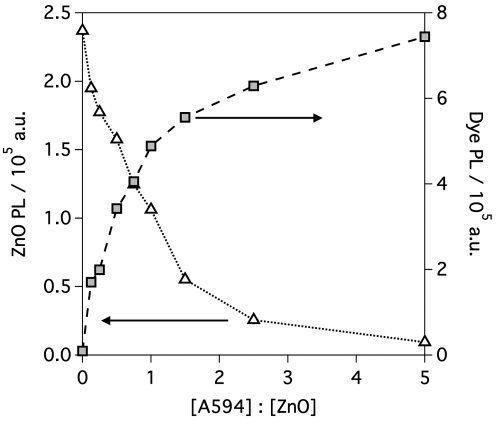

Figure 3. Photoluminescence (PL) of solutions containing 212 nM zinc oxide with increasing concentrations of A594 cadaverine in ethanol. Left (empty triangles): the defect emission at 510 nm with increasing A594/ZnO ratio; right (squares): the dye emission at 610 nm.

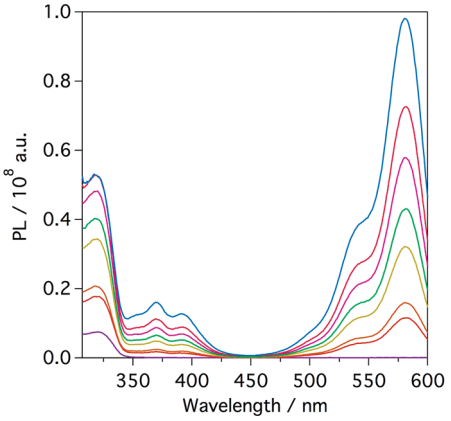

Figure 4. Excitation spectra of solutions of 212 nM ZnO with increasing concentrations of A594 cadaverine from 0 to 1060 nM in ethanol from bottom to top. Emission was detected at a wavelength of 610 nm.

of 3.2 nm.[12] Whereas typical semiconductor nanoparticles have significant exciton emission, the ZnO emission spectrum is dominated by defect emission centered at 510 nm, with no evidence of the exciton emission. The A594 cadaverine dye has an absorbance maximum at 591 nm, whereas the emission spectrum is Stokes shifted by 19 nm with a maximum at 610 nm. The dye absorbs little around 314 nm, allowing a window for the selective excitation of the ZnO nancrystals. At the highest concentration of A594 cadaverine used here, the absorbance of the dye at 314 nm was 3×10^{-3}. Resonance energy transfer requires a spectral overlap between the donor emission and the acceptor absorbance spectra. It is evident from Figure 1 that there is significant spectral overlap of the ZnO defect emission with the absorption spectrum of the A594 cadaverine dye. In contrast the overlap between the exciton emission of ZnO and the dye absorbance is negligible.

Steady-State Emission. The emission spectra of ZnO solutions containing increasing concentrations of A594 cadaverine from 0 to 1060 nM are displayed in Figure 2. It is evident from this Figure and from Figure 3 that as the concentration of the dye is increased the intensity of the defect emission decreases and the intensity of the dye emission increases concomitantly. For all dye

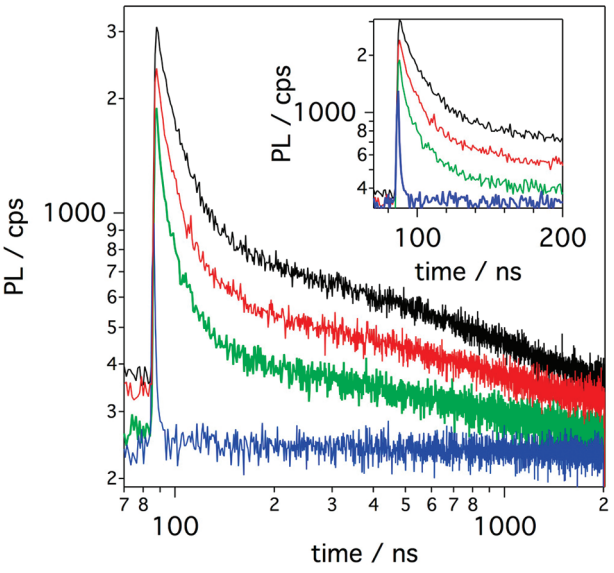

Figure 5. PL decay of 212 nM ZnO and with 0.5 (red), 1.0 (green), and 5.0 (blue) stoichiometric equivalents of A594 cadaverine dye in ethanol. Inset: The PL decay of the four ZnO solutions during the first 200 ns. Excitation was with 300 nm wavelength light and detected at 500 nm.

additions, the ZnO exciton emission remains absent. The increase in the dye emission is not due to direct excitation of the dye because the dye emission is more than an order of magnitude weaker than the ZnO emission at the excitation wavelength (Supporting Information Figures 1 and 2). The presence of an isosbestic point in Figure 2 and the lack of any significant change in the absorbance of the ZnO at 314 nm (Supporting Information Figure 3) provide further evidence (i) that there is no aggregation of the ZnO NCs due to the addition of dye, (ii) that the decrease in the ZnO defect state emission is not due to electron transfer (as the sum of the dye and ZnO absorbance spectra is the same as the mixed solution), and (iii) that the quenching originates from a single process, which we ascribe to energy transfer. The excitation spectrum of A594 cadaverine in the presence and absence of ZnO is shown in Figure 4. In the absence of ZnO, the excitation spectrum (monitored at 610 nm) is characteristic of A594 cadaverine with an intense maximum at 590 nm (Supporting Information Figure 2). After the addition of ZnO, which does not fluoresce significantly at 610 nm, the excitation spectrum exhibits features characteristic of the ZnO exciton state. This indicates that the emission at 610 nm is occurring upon excitation of the ZnO and allows us to conclude unequivocally that energy transfer takes place from the ZnO to the dye.

The A594 cadaverine dye contains a primary amine, which is free to bind to the surface of the ZnO nanocrystals. As a control experiment to establish whether unbound dye could also quench ZnO PL, a dye with no amine capable of binding to the surface was used, Rh6G. This dye has a similar absorbance spectrum to A594 cadaverine along with a larger spectral overlap with the ZnO defect emission, but it has a much lower binding affinity for the particle surface. Consistent with this, we found that Rh6G does not quench the defect emission of ZnO nanocrystals nor is the emission of the dye enhanced under the conditions used for these experiments (Supporting Information Figures 4 and 5). Hence, only adsorbed dyes are active quenchers. To demonstrate that the interaction of the amine moiety with the surface of the

ZnO nanocrystals does not perturb the defect emission, aminopentanol was titrated into the colloid. There was no change in either the exciton or defect state emission over the concentration range used for the energy-transfer experiments (Supporting Information Figure 6). Hence, we conclude that the defect emission is quenched by adsorbed A594 cadaverine molecules only, and this effect is not due to changes to the surface chemistry of the ZnO nanocrystals.

The PL decay of 212 nM ZnO in the presence of increasing amounts of A594 cadaverine is shown in Figure 5. The ethanolic samples were excited using a pulsed laser at 300 nm with detection at 500 nm. The decay in the absence of dye appears to be roughly biexponential, as observed previously for ZnO.[21] Notably, the cadaverine quenches both the fast and slow luminescence processes.

DISCUSSION

Steady-State Quenching. Whereas previous studies of fluorescence resonance energy transfer (FRET) in QD systems have shown only that exciton-state energy can be rapidly transferred to neighboring or adsorbed dye molecules, the results here unequivocally demonstrate that even trapped charge carriers can transfer energy to fluorophores. However, the fact that the energy donor is a localized defect state within a nanocrystal complicates the use of dipole−dipole electric coupling models such as FRET. This is because the exact location of the defect, whether on the surface of the particle or the core, will be different for each particle-dye conjugate, and this in turn will result in a broad distribution of donor−acceptor distances.

To model the static quenching of CdSe NC exciton emission by adsorbed dye molecules, Funston et al. made several assumptions.[7] First, a Langmuir adsorption isotherm was used to allow for partitioning of the dye molecules between the solution and surface. Second, it was assumed that there was a Poisson distribution of the adsorbed dye molecules among the nanocrystals, and finally, it was assumed that even a single adsorbed molecule completely quenched the NC PL. Whereas this model was consistent with the quenching data provided (Stern−Volmer plot), lifetime measurements were not presented. More recently, Sadhu and Tachiya[1] have modified the micelle quenching model proposed by Tachiya in 1975[37] to account for both quenching and lifetime data in nanocrystal−fluorophore systems. This model likewise assumes both a Langmuir adsorption isotherm and a Poisson distribution of adsorbed dye molecules. However, it relaxes the assumption of complete quenching by a single fluorophore.

According to this model, dye quenching (k_q) occurs in competition with radiative decay k_0

$$\begin{aligned} &NC^* : \Delta_n \xrightarrow{k_0} NC : \Delta_n \\ &NC^* : \Delta_n \xrightarrow{n \cdot k_q} NC : \Delta^*_n \end{aligned} \tag{1}$$

Here $NC^*:\Delta_n$ is the excited NC with n ground-state adsorbed dye molecules (denoted by the symbol Δ), $NC:\Delta_n$ is the ground-state NC with ground-state dye molecules adsorbed (the excitation has not been transferred to the attached dye molecules(s)), and $NC:\Delta^*_n$ represents the system after energy transfer to one of the n adsorbed dye molecules has taken place. From eq 1, the total decay rate of the excited state is then $k_0 + n \cdot k_q$.

The number of dye molecules adsorbed to each NC can be described according to Poisson statistics, and consequently the PL decay is given by

$$\frac{I}{I_0} = \sum_{n=0}^{n \to \infty} \frac{e^{-\lambda_s} \lambda_s^n e^{-(k_0 + nk_q)t}}{n!} \tag{2}$$

where I is the intensity, I_0 is the PL intensity in the absence of fluorophores, $1/k_0$ is the radiative lifetime of the ZnO defect emission in the absence of the fluorophore, λ_s is the mean number of dye molecules adsorbed to the surface, and k_q is the rate of energy transfer to a single dye molecule. This equation can be further simplified by taking the terms independent of the index n outside of the summation

$$\begin{aligned} \frac{I}{I_0} &= e^{-k_0 t - \lambda_s} \sum_{n=0}^{n \to \infty} \frac{(\lambda_s e^{-k_q t})^n}{n!} \\ &= e^{-k_0 t - \lambda_s (1 - \exp(-k_q t))} \end{aligned} \tag{3}$$

However, as noted above, the decay of the ZnO defect emission does not obey single exponential kinetics. Because our goal here is to quantify how efficiently it can be quenched and we do not aim to explain the transitions responsible for the emission, it suffices to fit empirically the trap emission to a simple kinetic scheme that can reproduce the decay profile. We note first that the quantum yield of both exciton and trap emission is at most ~15%. Hence most electron-hole pairs in ZnO NCs are annihilated via nonradiative recombination. Second, the defect emission decay contains a fast and slow process (Figure 5), and the decay kinetics are almost independent of wavelength. These observations suggest that slow radiative decay rate k_0 of the defects competes with nonradiative quenching by inherent trap states. We will assume that these trap states have a mean number λ_t per nanocrystal and exhibit a quenching rate of k_{qt}. It transpires that we do not need many of these traps, so they are also distributed in a colloid according to the Poisson equation. Then, the PL decay of a ZnO NC ensemble is given by

$$\frac{I}{I_0} = \exp\left(-k_0 t - \lambda_t (1 - \exp(-k_{qt} t))\right) \tag{4}$$

The green ZnO emission can be well-fit to this equation and yields values of $k_0 = 0.0017\ ns^{-1}$, $\lambda_t = 1.98$, and $k_{qt} = 0.039\ ns^{-1}$. We stress that this model is used simply as a baseline from which to calculate the effects of the quencher molecules. Therefore, when there is quenching from both trap states and adsorbed dye molecules, the PL decay of the NC solution is given by

$$\frac{I}{I_0} = \exp\left(-k_0 t - \lambda_t (1 - \exp(-k_{qt} t)) - \lambda_s (1 - \exp(-k_q t))\right) \tag{5}$$

We can define the quenching efficiency (ϕ) as

$$\phi = \frac{k_q}{k_0 + k_q + k_{qt}} \tag{6}$$

The data in Figure 5 were fit to eq 5 to obtain values of λ_s and k_q. The fraction of dye molecules adsorded to the ZnO nanocrystals was then determined from the slope λ_s versus the number of stoichiometric equivalents added (Figure 6) and found to be 0.62. The mean value of the energy transfer rate constant was $k_q = 0.14\ ns^{-1}$, corresponding to a quenching efficiency of 80% per adsorbed dye molecule. It is evident from

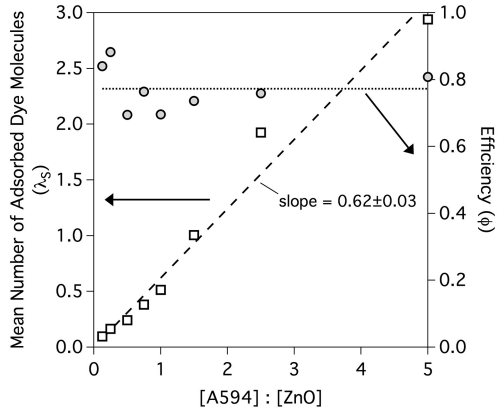

Figure 6. Analysis of the quenching data. Left axis: The mean number of adsorbed dye molecules per ZnO nanoparticle (using eq 5) versus the number of dye equivalents added (squares). Best fit to the data yields a slope of 0.62 ± 0.03 (dashed line). Right axis: The calculated quenching efficiency as a function of the number of dye equivalents added (circles). The data yield an efficiency of 77 ± 2%.

Figure 6 that the quenching efficiency is independent of the number of dye molecules adsorbed.

In summary, the fits show that the intrinsic rates of energy transfer from the ZnO defect state are of order 0.1 ns^{-1}, an order of magnitude faster than the intrinsic rate of PL decay. This value is also significantly faster than the rate constant needed to allow for nonradiative recombination. In agreement with the previous conclusions of Funston et al.,[7] that the nanocrystal exciton emission can be quenched by a single fluorophore, we now find that this applies to defect state emission too. This is all the more remarkable given the wide spread in donor−acceptor distances and dipole orientation in these systems.

It is worth noting that whereas other groups have reported the presence of two distinct defects (at approximately 500 and 570 nm, respectively),[38] the ZnO synthesized in this work exhibits only one defect (at 510 nm). Work by Shi et al.[39] and others[40] shows that despite the visible emission from zinc oxide particles being quite broad, it can be modeled using the Huang−Rhys equation, which describes the coupling of an electronic state with a vibrational state. The defect emission of the ZnO NCs synthesized in this work is also accurately fit by the Huang−Rhys model in which only the amplitude factor changes with dye addition. (See the Supporting Information.) This implies that defect emission in ZnO involves a single electronic transition that strongly couples to the phonon modes of the crystal lattice and not a distribution of trap states.

The uniform decrease in the emission of the ZnO in our experiments upon A594 cadaverine addition, even those parts of the spectrum that do not overlap with the dye, demonstrates that the defect emission behaves as a single (donor) state rather than a series of discrete trap states. Recent single-particle experiments by Layek and coworkers[41] further support these findings and demonstrate that the broad emission is from coupling of the excited state and the phonon modes rather than polydispersity.

CONCLUSIONS

We have demonstrated that very efficient energy transfer occurs from ZnO nanocrystal defect states to adsorbed A594 cadaverine dye molecules. Steady-state observations reveal that the addition of conjugated dye molecules results in the reduction of defect emission, without changing the line shape. Time-resolved measurements demonstrate that the energy transfer in this system is from the defect state, with the apparent lifetime of both components of the ZnO fluorescence decay decreasing with increasing stoichiometric equivalents of dye. This change in the apparent lifetime was fit using the Sadhu kinetic model, further supporting the use of Poisson statistics in analyzing energy transfer in the present system. This work illustrates that defect states in nanocrystals must be considered in energy transfer assays, not just exciton states, as defects themselves can undergo energy transfer to acceptor molecules.

ASSOCIATED CONTENT

Supporting Information. PL spectra and excitation spectra of solutions; absorbance spectra for titration of A594 cadaverine; emission spectra of solutions with increasing proportions of Rhodamine 6G, plot of the PL of the ZnO defect at 510 nm with the addition of aminopentanol (AP) into an ethanolic solution, and the PL decay of a 212 nM ZnO solution in ethanol. This material is available free of charge via the Internet at http://pubs.acs.org.

AUTHOR INFORMATION

Corresponding Author
*E-mail: mulvaney@unimelb.edu.au.

ACKNOWLEDGMENT

This work was supported by the Australian Research Council via grants LF100100117 and DP0985325. A.J.M. acknowledges the support of the Melbourne Materials Institute.

REFERENCES

(1) Sadhu, S.; Tachiya, M. *J. Phys. Chem.* **2009**, *113*, 19488–19492.
(2) Clapp, A. R.; Medintz, I. L.; Mauro, J. M.; Fisher, B. R.; Bawendi, M. G.; Mattoussi, H. *J. Am. Chem. Soc.* **2004**, *126*, 301–310.
(3) Clapp, A. R.; Medintz, I. L.; Mattoussi, H. *ChemPhysChem* **2006**, *7*, 47–57.
(4) Medintz, I. L.; Sapsford, K. E.; Clapp, A. R.; Pons, T.; Higashiya, S.; Welch, J. T.; Mattoussi, H. *J. Phys. Chem. B* **2006**, *110*, 10683–10690.
(5) Pons, T.; Medintz, I. L.; Sykora, M.; Mattoussi, H. *Phys. Rev. B* **2006**, *73*, 245302.
(6) Soujon, D.; Becker, K.; Rogach, A. L.; Feldmann, J.; Weller, H.; Talapin, D. V.; Lupton, J. M. *J. Phys. Chem. C* **2007**, *111*, 11511–11515.
(7) Funston, A. M.; Jasieniak, J. J.; Mulvaney, P. *Adv. Mater.* **2008**, *20*, 4274–4280.
(8) Bera, D.; Qian, L.; Sabui, S.; Santra, S.; Holloway, P. H. *Opt. Mat.* **2008**, *30*, 1233–1239.
(9) Morfa, A. J.; Beane, G.; Mashford, B.; Singh, B.; Della Gaspera, E.; Martucci, A.; Mulvaney, P. *J. Phys. Chem. C* **2010**, *114*, 19815–19821.
(10) Spanhel, L.; Anderson, M. A. *J. Am. Chem. Soc.* **1991**, *113*, 2826–2833.
(11) van Dijken, A.; Meulenkamp, E. A.; Vanmaekelbergh, D.; Meijerink, A. *J. Phys. Chem. B.* **2000**, *104*, 1715−1723.
(12) Wood, A.; Giersig, M.; Hilgendorff, M.; Vilas-Campos, A.; Liz-Marzan, L. M.; Mulvaney, P. *Aust. J. Chem.* **2003**, *56*, 1051–1057.
(13) Mollwo, E. Z. *Z. Phys.* **1954**, *138*, 478–488.
(14) Kroger, F. A.; Vink, H. J. *J. Phys. Chem.* **1954**, *22*, 250–252.
(15) Vancraey, F.; Maenhout, W.; Dekeyser, W. *Phys. Status Solidi* **1965**, *8*, 841.
(16) Dingle, R. *Phys. Rev. Lett.* **1969**, *23*, 579–581.
(17) Smith, J. M.; Vehse, W. E. *Phys. Lett. A* **1970**, *31*, 147–148.

(18) Anpo, M.; Kubokawa, Y. *J. Phys. Chem.* **1984**, *88*, 5556–5560.
(19) Vanheusden, K.; Seager, C. H.; Warren, W. L.; Tallant, D. R.; Voigt, J. A. *Appl. Phys. Lett.* **1996**, *68*, 403–405.
(20) Vanheusden, K.; Warren, W. L.; Seager, C. H.; Tallant, D. R.; Voigt, J. A.; Gnade, B. E. *J. Appl. Phys.* **1996**, *79*, 7983.
(21) van Dijken, A.; Meulenkamp, E. a.; Vanmaekelbergh, D.; Meijerink, A. *J. Phys. Chem. B* **2000**, *104*, 1715–1723.
(22) Ozgür, U.; Alivov, Y. I.; Liu, C.; Teke, A.; Reshchikov, M. A.; Dogan, S.; Avrutin, V.; Cho, S. J.; Morkoc, H. *J. Appl. Phys.* **2005**, *98*, 041301 .
(23) Yu, H.-h.; Wong, M. K. F.; Ali, E. M.; Ying, J. Y. *Chem. Commun.* **2008**, 4912–4914.
(24) Rakshit, S.; Vasudevan, S. *ACS Nano* **2008**, *2*, 1473–1479.
(25) Park, J. K.; Lee, K. W.; Lee, W.; Lee, C. E. *Appl. Phys. Lett.* **2009**, *94*, 233301–233301.
(26) Makhal, A.; Sarkar, S.; Bora, T.; Baruah, S.; Dutta, J.; Raychaudhuri, a. K.; Pal, S. K. *Nano*. **2010**, *21*, 265703-1−265703-5.
(27) Makhal, A.; Sarkar, S.; Bora, T.; Baruah, S.; Dutta, J.; Raychaudhuri, a. K.; Pal, S. K. *J. Phys. Chem. C* **2010**, *114*, 10390–10395.
(28) Bahnemann, D. W.; Kormann, C.; Hoffmann, M. R. *J. Phys. Chem.* **1987**, *91*, 3789–3798.
(29) Li, D.; Leung, Y. H.; Djurisic, A. B.; Liu, Z. T.; Xie, M. H.; Shi, S. L.; Xu, S. J.; Chan, W. K. *Appl. Phys. Lett.* **2004**, *85*, 1601–1603.
(30) Norberg, N. S.; Gamelin, D. R. *J. Phys. Chem. B* **2005**, *109*, 20810–20816.
(31) Singla, M. L.; M, M. S.; Kumar, M. *J. Lumin.* **2009**, *129*, 434–438.
(32) Bullen, C.; Mulvaney, P. *Langmuir* **2006**, *22*, 3007–3013.
(33) Noto, Y.; Fukuda, K.; Onishi, T.; Tamaru, K. *Trans. Faraday Soc.* **1967**, *63*, 3081.
(34) Curri, M. L.; Comparelli, R.; Cozzoli, P. D.; Mascolo, G.; Agostiano, A. *Mater. Sci. Eng., C* **2003**, *23*, 285–289.
(35) Kubin, R. F.; Fletcher, A. N. *J. Lumin.* **1982**, *27*, 455–462.
(36) Fluorescence Quantum Yields (QY) and Lifetimes (t) for Alexa Fluor Dyes - Table 1.5. In *Molecular Probes Handbook, a Guide to Fluorescent Probes and Labeling Technologies, 11th ed*; Invitrogen, 2010.
(37) Tachiya, M. *Chem. Phys. Lett.* **1975**, *33*, 289–292.
(38) Rakshit, S.; Vasudevan, S. *J. Phys. Chem. C* **2009**, *113*, 16424–16431.
(39) Shi, S. L.; Li, G. Q.; Xu, S. J.; Zhao, Y.; Chen, G. H. *J. Phys. Chem. B* **2006**, *110*, 10475–10478.
(40) Reynolds, D. C.; Look, D. C.; Jogai, B. *J. Appl. Phys.* **2001**, *89*, 6189–6191.
(41) Layek, A.; De, S.; Thorat, R.; Chowdhury, A. *J. Phys. Chem. Lett.* **2011**, *2*, 1241–1247.